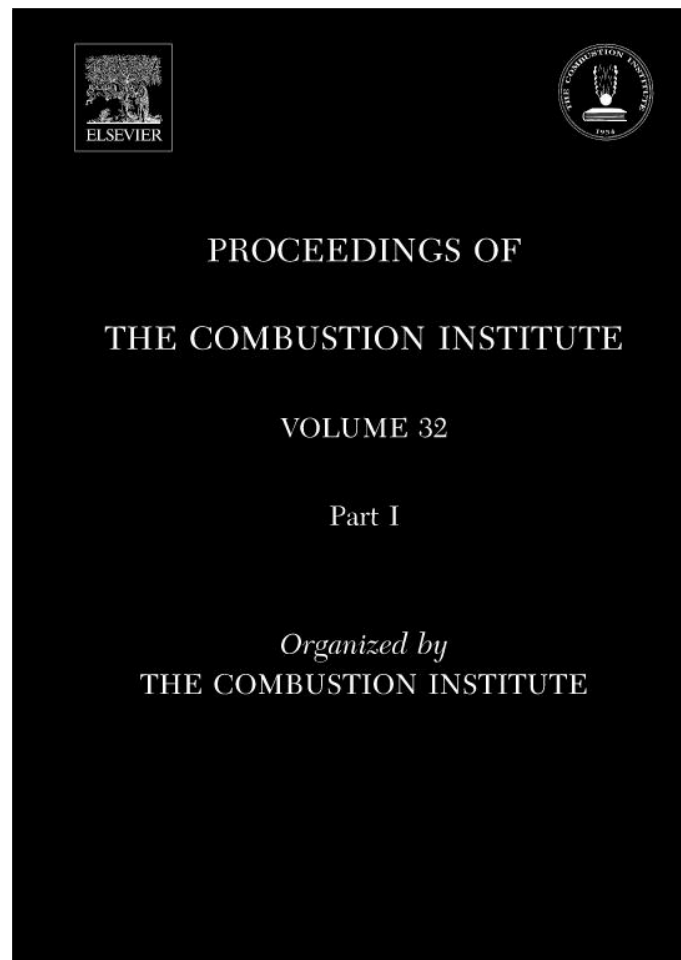


Provided for non-commercial research and education use.  
Not for reproduction, distribution or commercial use.



This article appeared in a journal published by Elsevier. The attached copy is furnished to the author for internal non-commercial research and education use, including for instruction at the authors institution and sharing with colleagues.

Other uses, including reproduction and distribution, or selling or licensing copies, or posting to personal, institutional or third party websites are prohibited.

In most cases authors are permitted to post their version of the article (e.g. in Word or Tex form) to their personal website or institutional repository. Authors requiring further information regarding Elsevier's archiving and manuscript policies are encouraged to visit:

<http://www.elsevier.com/copyright>



ELSEVIER

Available online at [www.sciencedirect.com](http://www.sciencedirect.com) ScienceDirect

Proceedings of the Combustion Institute 32 (2009) 247–253

---

---

**Proceedings  
of the  
Combustion  
Institute**

---

---

[www.elsevier.com/locate/proci](http://www.elsevier.com/locate/proci)

# An experimental and computational study of methyl ester decomposition pathways using shock tubes

A. Farooq<sup>a</sup>, D.F. Davidson<sup>a,\*</sup>, R.K. Hanson<sup>a</sup>, L.K. Huynh<sup>b</sup>, A. Violi<sup>b</sup><sup>a</sup> *Mechanical Engineering Department, Stanford University, Building 520, Duena Street, Stanford, CA 94305, USA*<sup>b</sup> *University of Michigan, Ann Arbor, MI 48109, USA*

---

## Abstract

The high-temperature decomposition of three simple methyl esters: methyl acetate, methyl propionate and methyl butanoate, were studied behind reflected shock waves using tunable diode laser absorption of CO<sub>2</sub> near 2.7 μm. CO<sub>2</sub> yield measurements were made over the range of temperatures 1260–1653 K, pressures of 1.4–1.7 atm and reactant concentrations of 2–3%, with the balance Ar. The CO<sub>2</sub> absorption strengths near 2.7 μm are approximately 50 to 1000 times stronger than the bands near 2.0 and 1.55 μm, respectively, and offer opportunities for significantly more sensitive and accurate combustion measurements than previous absorption work using CO<sub>2</sub> bands at shorter wavelength. The experiments provide the first laser-based time-history measurements of the CO<sub>2</sub> yields during pyrolysis of these bio-diesel surrogate fuels in a shock tube. Model predictions for CO<sub>2</sub> yields during methyl butanoate pyrolysis at high temperatures, using the detailed reaction mechanisms of [E. M. Fisher, W. J. Pitz, H. J. Curran, C. K. Westbrook, *Proc. Combust. Inst.* 28 (2000) 1579–1586.] and others, are significantly lower than those measured in this study. However, an improved methyl butanoate model which extends the recent theoretical work of [L.K. Huynh, A. Violi, *J. Org. Chem.* 73 (2008) 94–101.] provides substantially improved predictions of CO<sub>2</sub> yields during methyl butanoate pyrolysis. As earlier mechanisms predicted low yields of CO<sub>2</sub> from methyl butanoate decomposition, these new findings imply that existing bio-diesel fuel models, which rely on the rapid formation of two oxygenate radicals from methyl esters (rather than a single non-reactive CO<sub>2</sub> molecule) to account for the tendency for soot reduction, may have to be revisited.

© 2009 The Combustion Institute. Published by Elsevier Inc. All rights reserved.

*Keywords:* Methyl ester; Methyl butanone; Shock tube; Laser absorption; CH<sub>3</sub>OCO Decomposition

---

## 1. Introduction

The use of bio-diesel fuels as replacements or supplements for crude-oil-derived diesel fuel addresses two of the major concerns about current diesel supplies, namely greenhouse gas emissions and sulfur content. Bio-diesel offers the advantage of a renewable fuel with little added

atmospheric CO<sub>2</sub> greenhouse burden and the advantage of a clean fuel with a low potential to form SO<sub>x</sub>. It has also been shown that bio-diesel fueled engines can produce less CO and unburned hydrocarbons particularly when compared to diesel fuel [1]. Derivable from vegetable oils and animal fats, bio-diesels usually take the form of long-chain methyl esters. High-temperature shock tube studies of methyl ester pyrolysis and oxidation can provide kinetic targets needed to refine and validate detailed mechanisms for these fuels.

---

\* Corresponding author.

E-mail address: [dfd@stanford.edu](mailto:dfd@stanford.edu) (D.F. Davidson).

These long-chain methyl esters, while directly compatible with diesel operation, are generally difficult to study in the laboratory because of their low vapor pressure and chemical complexity. Methyl butanoate,  $\text{CH}_3\text{CH}_2\text{CH}_2\text{CO}_2\text{CH}_3$  (MB) has been used as a surrogate for long-chain methyl esters by several researchers [2–5] because it contains much of the essential chemical structure of its long-chain counterparts, i.e., the methyl ester termination and a shorter, but similar alkyl chain, and because detailed reaction mechanisms describing this fuel are of a manageable size. Comprehensive detailed mechanisms for methyl esters can be large, not only because of the complexity of these molecules, but also because of the large complement of oxygen addition-related reactions needed to describe low-temperature ignition; e.g., a recent mechanism for methyl decanoate ignition contains 3012 species and 8820 reactions [6]. Because of this difference between surrogate and bio-diesel molecule size, information is also needed on the influence of structure and chain length on methyl ester kinetics.

If studies are limited to high temperatures, a smaller reaction mechanism may be sufficient to describe the chemistry, and the influence of the important decomposition and H-abstraction reactions can be studied more directly. However, little data on species concentration time-histories are available at high temperatures in the methyl ester systems, particularly from shock tubes. If these data were available, they would provide strong constraints on proposed methyl ester decomposition pathways and rates and on overall detailed reaction mechanisms. The time-history of one species,  $\text{CO}_2$ , is particularly important in methyl ester decomposition. Its occurrence in high-temperature pyrolysis systems can be directly related to the magnitude of the reaction rates of the decomposition pathways which directly form  $\text{CO}_2$  and do not separate the two oxygen atoms in a methyl ester into two separate CO-carrying intermediate products.

Current model predictions for CO and  $\text{CO}_2$  yields in MB pyrolysis at high temperatures, using for example the detailed reaction mechanism of Fisher et al. [2], show a partitioning that favors some CO yield pathways. A consequence of this partitioning is that at high temperatures, methyl ester bio-diesel fuel surrogate molecules decompose into two reactive oxygenate intermediates. These reactive oxygenate intermediates are assumed to contribute to the tendency of methyl esters to reduce sooting in engines that is evident with bio-diesel fuels [7,8]. However, more recent studies by Westbrook et al. [7] and Gail et al. [4] suggest that the decomposition partitioning favors  $\text{CO}_2$  rather than CO-carrying intermediates. If  $\text{CO}_2$  formation is strongly favored, it may suggest that current interpretations of the role of methyl esters in reducing soot would have to be revisited.

We are aware of no high-temperature, shock tube studies of the  $\text{CO}_2$  yields from the smaller methyl ester, methyl propionate,  $\text{CH}_3\text{CH}_2\text{CO}_2\text{CH}_3$  (MP). However, Sulzmann et al. [9] did investigate the rate of  $\text{CO}_2$  and  $\text{CH}_3$  formation during methyl acetate,  $\text{CH}_3\text{CO}_2\text{CH}_3$  (MA) pyrolysis in a shock tube using infrared emission and ultraviolet lamp absorption. Their study found that at low initial concentrations (0.1% and 0.5%), temperatures of 1425 to 1844 K, and pressures of 1.2 to 5.6 atm, methyl acetate decomposed nearly completely to  $\text{CO}_2$  and  $2\text{CH}_3$ . We are unaware of any published mechanisms for MA or MP decomposition.

In the present study, we have measured  $\text{CO}_2$  time-histories during the pyrolysis of three methyl esters: methyl acetate,  $\text{CH}_3\text{CO}_2\text{CH}_3$ ; methyl propionate,  $\text{CH}_3\text{CH}_2\text{CO}_2\text{CH}_3$ ; and methyl butanoate,  $\text{CH}_3\text{CH}_2\text{CH}_2\text{CO}_2\text{CH}_3$ . These three methyl esters are identical except for their chain length (i.e., have the same degree of saturation.) These measurements are performed at higher concentrations (2–3%), where secondary reactions (i.e., H-abstraction reactions) are important. To model these experiments, we have developed an improved MB model based on the theoretical work of Huynh and Violi [5] that includes an *ab initio* study of MB pyrolysis reactions.

The measurements are carried out behind reflected shock waves using a new class of room-temperature tunable diode lasers near 2.7  $\mu\text{m}$ . The probed transition belongs to the  $\nu_1 + \nu_3$  combination band of  $\text{CO}_2$  that has stronger absorption linestrengths than the bands near 1.5 and 2.0  $\mu\text{m}$  used previously to sense  $\text{CO}_2$  in combustion gases. Specifically, the band near 2.7  $\mu\text{m}$  is approximately 50 to 1000 times stronger than the bands near 2.0  $\mu\text{m}$  ( $\nu_1 + 2\nu_2 + \nu_3$ ) and 1.55  $\mu\text{m}$  ( $2\nu_1 + 2\nu_2 + \nu_3$ ), respectively. The increased absorption strengths of transitions in this wavelength region thus offer opportunities for more sensitive and accurate combustion measurements than previous work using the  $\text{CO}_2$  bands at shorter wavelength [10,11].

## 2. Experimental details

Experiments were performed in the reflected shock region of a high-purity, stainless-steel, helium-driven shock tube regularly used in our laboratory for kinetics studies [12,13]. The driven section is 8.54 m long and the driver section 3.35 m long; both sections have an inner diameter of 14.13 cm. This geometric configuration provided at least 2 ms of high-quality test time of uniform temperature and pressure for these studies. The temperature and pressure behind the reflected shock waves were calculated using standard normal shock relations and the measured incident shock speed. The incident shock speeds were

determined from time interval measurements from a series of 5 pressure transducers spread over the final 1 m of the shock tube and linearly extrapolated to the shock tube endwall. Prior to each experiment, the shock tube was evacuated by a turbomolecular pump to an ultimate pressure of  $\sim 3 \times 10^{-6}$  torr and a leak and outgassing rate of  $\sim 10^{-5}$  torr/min and then filled with a methyl ester/Ar mixture to a pre-shock pressure  $P_1$  of 20–50 torr. Commercially available methyl esters (>99% pure) from Sigma–Aldrich and research grade argon and helium supplied by Praxair Inc. were used in the experiments. Mixtures were prepared by partial pressures in a stainless steel mixing chamber equipped with a magnetic stirrer assembly and allowed to mix overnight. The mixing assembly and shock tube driven section were maintained at room temperature.

Absorption measurements of  $\text{CO}_2$  were made at a location 2 cm from the shock tube endwall. A fixed-wavelength direct-absorption strategy was used, providing a sensor bandwidth of about 1 MHz. Line-strength, self-broadening and Ar-broadening coefficients were measured previously for the R(28) transition (at 2752.5 nm) used. Ability to make accurate measurements of  $\text{CO}_2$  concentration has previously been demonstrated in  $\text{CO}_2$ –Ar mixtures over a temperature range of 300–1500 K [10,11]. The line-center absorption coefficient-pressure product,  $k_v \times P_{\text{total}}$ , is plotted in Fig. 1 for the R(28) transition as a function of temperature for two pressures, 1 and 2 atm. Quantitative  $\text{CO}_2$  concentration profiles are generated from the raw traces of fractional absorption using Beer's law and the known absorption coefficient [11]:

$$I/I_0 = \exp(-k_v P_{\text{total}} X_{\text{CO}_2} L). \quad (1)$$

where  $I$  and  $I_0$  are the transmitted and incident beam intensities,  $k_v$  is the line-center absorption coefficient at 2752.5 nm,  $P_{\text{total}}$  is the total test

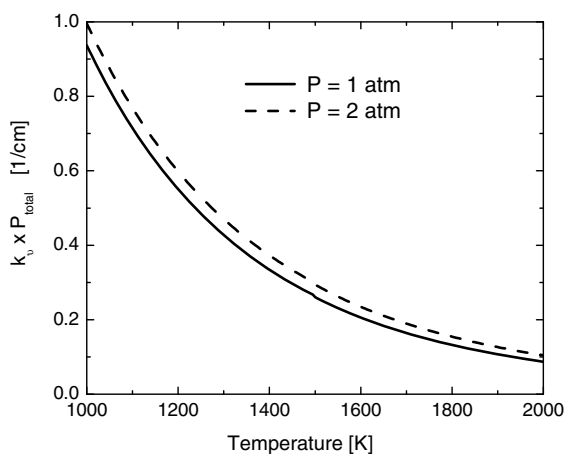


Fig. 1. Absorption coefficient  $\times$  pressure product,  $k_v \times P_{\text{total}}$  [ $\text{cm}^{-1}$ ] for the R(28)  $\text{CO}_2$  transition near  $3633.08 \text{ cm}^{-1}$  ( $2752.5 \text{ nm}$ ) at  $P = 1$  and  $2 \text{ atm}$ .

gas mixture pressure,  $X_{\text{CO}_2}$  is the desired quantity, i.e., mole fraction of  $\text{CO}_2$ , and  $L$  is the pathlength, 14.13 cm in the current experiments.

Experiments were also conducted at wavelengths away from the  $\text{CO}_2$  transition to test for any absorption interference. Small levels of absorption interference were observed in methyl butanoate and methyl acetate pyrolysis, while there was negligible interference for methyl propionate pyrolysis. The off-line absorption was subtracted from the on-line absorption to obtain the actual absorption by  $\text{CO}_2$  for methyl butanoate and methyl acetate pyrolysis. A sample case is shown in Fig. 2 for a 2% MB/Ar mixture at  $T = 1426 \text{ K}$ ,  $P = 1.58 \text{ atm}$ . Measurement uncertainties are quite small (<3%) and come from uncertainties in the measured spectral database (2% in linestrength, 2.5% in Ar-broadening) and the reflected shock temperature (<1%).

### 3. Results and discussion

Pyrolysis experiments of methyl esters in argon were conducted at temperatures from 1260 to 1653 K and at pressures from 1.4 to 1.7 atm. MB and MP experiments were performed with 2% mixtures, while the MA experiments were performed with 3% mixtures. The measured time-histories of  $\text{CO}_2$  concentration are plotted in Figs. 3–5 for methyl acetate, methyl propionate and methyl butanoate, respectively.

The  $\text{CO}_2$  fractional yield for each methyl ester at 1 ms is plotted as a function of temperature in Fig. 6.  $\text{CO}_2$  yields exceed 50% at temperatures above 1500 K for all three methyl esters. There does not appear to be a strong relationship between the  $\text{CO}_2$  yield and the length of the alkyl

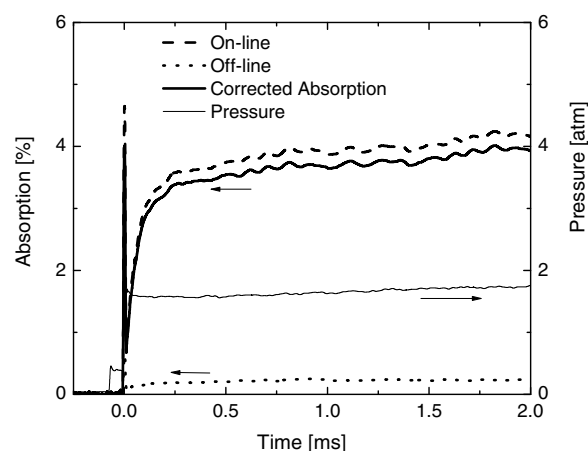


Fig. 2. Example on-line and off-line absorption measurement in 2% MB/Argon. Reflected shock conditions:  $T_5 = 1426 \text{ K}$ ,  $P_5 = 1.58 \text{ atm}$ . On-line wavenumber =  $3633.08 \text{ cm}^{-1}$ ; Off-line wavenumber =  $3633.25 \text{ cm}^{-1}$ .

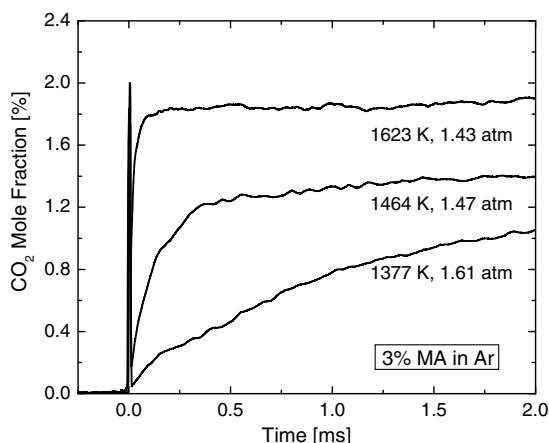


Fig. 3. Measured  $\text{CO}_2$  time-histories behind reflected shock waves ( $T_5$ ,  $P_5$  shown) for methyl acetate pyrolysis (3% MA in Ar).

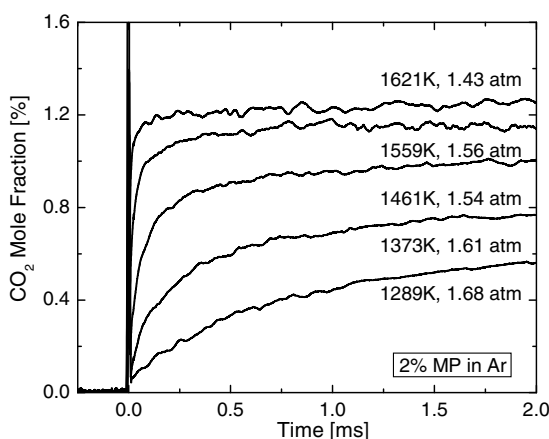


Fig. 4. Measured  $\text{CO}_2$  time-histories behind reflected shock waves ( $T_5$ ,  $P_5$  shown) for methyl propionate pyrolysis (2% MP in Ar).

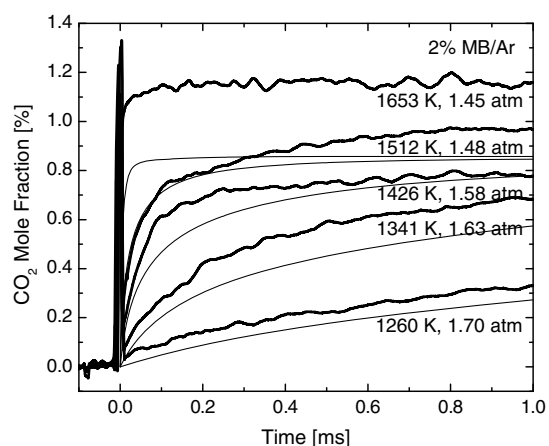


Fig. 5. Calculated (light solid) and measured (heavy solid)  $\text{CO}_2$  concentration time histories for methyl butanoate pyrolysis (2% MB in Ar).  $\text{CO}_2$  profiles were calculated using the improved MB model of the current study.

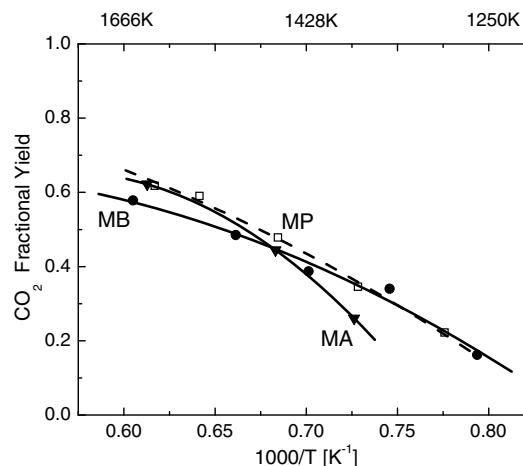


Fig. 6. Measured  $\text{CO}_2$  fractional yields at 1 ms. Pressure: 1.4–1.7 atm.

chain for these three smaller methyl esters. However, there is some evidence that the  $\text{CO}_2$  yield for MA at the lowest temperature measured, 1377 K, is lower (by 25%) than that observed for MP or MB. Sulzmann et al. [9] found  $\text{CO}_2$  yields of 100% for MA at low concentrations at temperatures of 1425 to 1844 K. This difference may be related to the increased role of secondary reactions in the present study. A fuller investigation of this difference must wait for the development of detailed kinetic mechanisms for MA (and MP).  $\text{CO}_2$  yields in the MB experiments are discussed in the next section.

### 3.1. An improved MB model

The chemical kinetic analysis of the current methyl butanoate data uses an improved MB model. Using *ab initio* methods Huynh and Violi [5] developed an MB pyrolysis sub-model that includes two main parts: the 13 methyl butanoate pyrolysis pathways (47 reactions in total); and a recalculated rate for  $\text{CH}_3\text{OCO}$  dissociation and recombination channels. The rates for the unimolecular and bimolecular reactions in these pyrolysis pathways were calculated using a BH&HLYP/cc-pVTZ potential energy surface and Rice–Ramsperger–Kassel–Marcus (RRKM) and transition state theory (TST) theories, respectively. Corrections for hindered rotation and tunneling treatments were also included in the calculated rate constants. Rates for the  $\text{CH}_3\text{OCO}$  dissociation and recombination channels were recalculated using higher levels of theory (see section 3.2). This MB pyrolysis sub-model is embedded into the Fisher et al. [2] mechanism which is a larger reaction set framework. The Fisher et al. mechanism includes 264 species and 1219 reactions and, in particular, identified and estimated reaction rates for 9 decomposition pathways for MB. The MB pyrolysis pathways described by Huynh and Violi

replace related reaction pathways in the Fisher et al. framework. The improved MB model and associated thermochemistry will be available for download [14].

Two other recent studies have also attempted to improve and refine the Fisher et al. mechanism: Metcalfe et al. [3] and Gail et al. [4]. Predictions of these studies are also included in the following discussion. The CHEMKIN abbreviations used by Fisher et al. for selected MB-related radical species are given in parentheses.

Using the improved MB model, rate-of-production (ROP) and sensitivity analyses for CO<sub>2</sub> were performed. The results are presented in Figs. 7 and 8, respectively, at one of the experimental conditions (1426 K, 1.58 atm). The ROP analysis indicates that at 1426 K, there are two dominant pathways for the formation of CO<sub>2</sub>: through MB decomposition, Rxn. 1 followed by Rxn. 2; and through one of the CH<sub>3</sub>OCO decomposition pathways, Rxn. 3. CH<sub>3</sub>OCO is formed primarily by Rxns. 5 and 6.

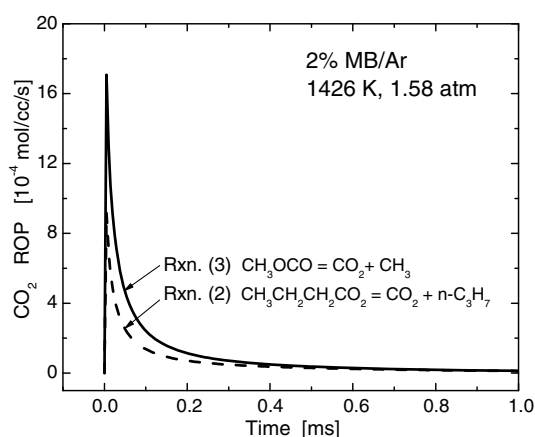


Fig. 7. Rate of production (ROP) for CO<sub>2</sub> as a function of time at initial conditions of 1426 K, 1.58 atm, 2% MB in argon.

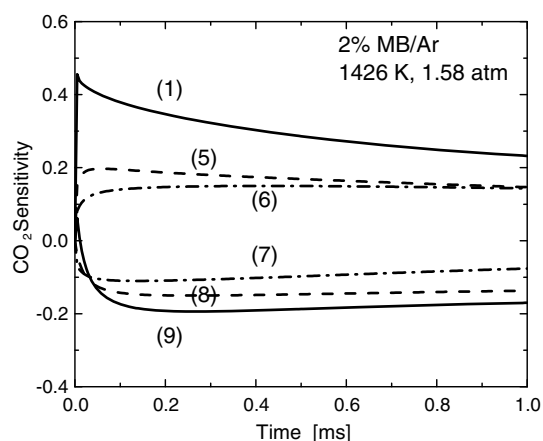
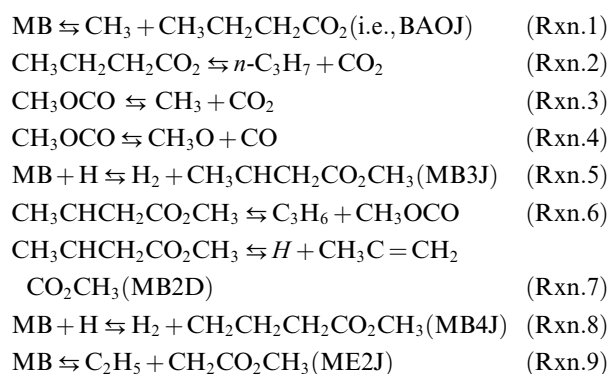


Fig. 8. Sensitivity analysis for CO<sub>2</sub> as a function of time at initial conditions of 1426 K, 1.58 atm, 2% MB in argon. The six largest sensitivities are shown.



The sensitivity analysis supports the ROP interpretation. The concentration of CO<sub>2</sub> is strongly sensitive to the initial decomposition of MB through Rxn. 1, which forms CO<sub>2</sub>, and to a lesser degree to Rxn. 9, whose products decompose to form two separate oxygen-carrying moieties. The CO<sub>2</sub> concentration is also relatively sensitive to two of the MB + H reactions: Rxns. 5 and 8. Reaction 8 does not directly lead to CO<sub>2</sub> production, but rather again to two separate oxygen-carrying moieties. Reaction 5 produces CH<sub>3</sub>CHCH<sub>2</sub>CO<sub>2</sub>CH<sub>3</sub>, which can decompose in one of two ways: Rxns. 6 and 7. The competition between these two pathways determines how much CH<sub>3</sub>OCO is formed. In the improved MB model, CH<sub>3</sub>OCO decomposes through Rxn. 3 into CH<sub>3</sub> + CO<sub>2</sub>. In the other detailed mechanisms [2–4], the relative rate of Rxn. 4 (to Rxn. 3) was larger than proposed in the improved MB model and thus competition between Rxn. 4 and 3 (the next two largest sensitivities, not shown in Fig. 8) limited the formation of CO<sub>2</sub> by the competing formation of CO by Rxn. 4.

Comparisons of the measured and modeled CO<sub>2</sub> yields for MB are shown in Figs. 5 and 9. The improved MB model closely approximates the CO<sub>2</sub> yields for temperatures up to about

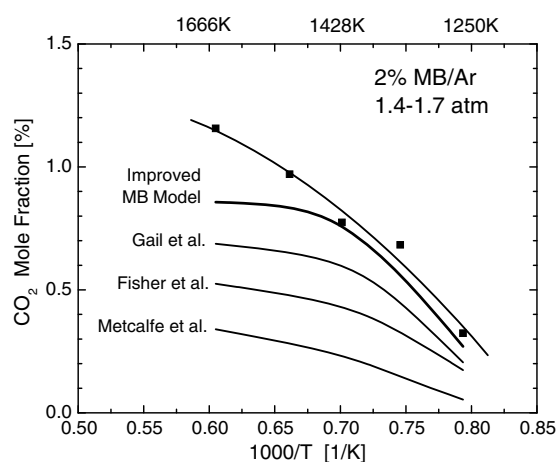


Fig. 9. Calculated and measured CO<sub>2</sub> fractional yields at 1 ms for 2% MB in Ar. The calculations use the improved MB model (Huynh and Violi), Fisher et al. [2], Metcalfe et al. [3] and Ga et al. [4] mechanisms.

1530 K, and then at higher temperatures begins to fall below the measurements. The predicted CO<sub>2</sub> yields from the other three mechanisms are significantly lower at all temperatures, with the deviation greatest at highest temperatures. The measured plateau values are approximately twice those of the original Fisher et al. mechanism. CO<sub>2</sub> concentration time-histories predicted using the more recent Metcalfe et al. [3] mechanism are even lower, typically one third of the measured values; and the CO<sub>2</sub> yields predicted using the Gail et al. [4] mechanism are approximately three quarters of the measured values at temperatures up to 1430 K. Recent works by Westbrook et al. [7] and Gail et al. [4] have revised the earlier assumption that the decomposition partitioning favors CO-carrying intermediates. Westbrook et al. have suggested up to 78% and 90% CO<sub>2</sub> production, respectively, for two related compounds, dimethyl carbonate and dibutyl maleate. Our current results are in agreement with these authors and predict that CO<sub>2</sub> formation is strongly favored over CO in methyl ester decomposition.

Decomposition of methyl esters has also been studied in premixed and non-premixed flames. Osswald et al. [19] have measured about 50% CO<sub>2</sub> yield for methyl acetate in premixed, laminar flat flame using molecular-beam sampling and photoionization mass spectrometry. At an intermediate temperature of 1500 K, where most of the methyl acetate decomposes, our results also predict 50% CO<sub>2</sub> yield. Schwartz et al. [20] have studied the decomposition of MB in non-premixed flame and investigated the relative importance of unimolecular and bimolecular ester decomposition pathways.

### 3.2. CH<sub>3</sub>OCO decomposition

The rate-of-production demonstrates the critical importance of Rxn. 3, CH<sub>3</sub>OCO = CH<sub>3</sub> + CO<sub>2</sub>, in modeling the CO<sub>2</sub> yield. The reaction rate and branching ratio of CH<sub>3</sub>OCO decomposition has been discussed by Glaude et al. and McCunn et al. [15,16]. However, using the *ab initio* rates given by Glaude et al. in the Fisher et al. mechanism raises the CO<sub>2</sub> yield to values comparable with Gail et al., but still lower than the experimentally measured values.

Huynh and Violi [5,14] have recalculated accurate rate constants for Rxns. 3 and 4 for both forward and reverse directions. The potential energy surface for these reactions was obtained at a high level of theory. Particularly, the G3-method variant [7] (denoted as G3//B3LYP) using geometries and zero-point energies obtained from B3LYP density functional theory [B3LYP/6-31G(d)] was used to obtain accurate energetic data for these reactions. The variant is believed to give the energetic information within the chemical accuracy, e.g., 1.0 kcal/mol.

Rate constants for the forward and reverse direction of Rxn. 3 and 4 were calculated using the Rice–Ramsperger–Kassel–Marcus (RRKM) theory and the canonical variational transition state theory (CVT) methods, respectively, with the results shown in Eqs. (2)–(5). The tunneling effect was included into the rate constants using the one-dimensional Eckart method for RRKM and small curvature tunneling (SCT) methodology for CVT. Hindered rotation corrections for the rotations of the CH<sub>3</sub> group along the C(H<sub>3</sub>)–O bond in both the reactant (CH<sub>3</sub>OCO) and transition state (CH<sub>3</sub>–OCO), and of the CO group along the (CH<sub>3</sub>)O–C(O) bond in the transition state (CH<sub>3</sub>)O–C(O) are also incorporated in the calculated rate constants using the approach proposed by Ayala and Schlegel [17].

$$k_3 = 1.55 \times 10^{12} T^{0.514} \exp(-15182/RT) [\text{s}^{-1}] \quad (2)$$

$$k_{-3} = 2.92 \times 10^6 T^{1.650} \exp(-36591/RT) [\text{cm}^3 \text{mole}^{-1} \text{s}^{-1}] \quad (3)$$

$$k_4 = 7.37 \times 10^{12} T^{0.479} \exp(-23807/RT) [\text{s}^{-1}] \quad (4)$$

$$k_{-4} = 1.08 \times 10^7 T^{1.633} \exp(-5588/RT) [\text{cm}^3 \text{mole}^{-1} \text{s}^{-1}] \quad (5)$$

The rates for reaction (3) given here are very similar to those proposed by Glaude et al. while the rates for reaction (–3) are significantly slower. At 1400 K,  $k_3(\text{current study})/k_3(\text{Glaude et al.}) = 0.87$  and  $k_{-3}(\text{current study})/k_{-3}(\text{Glaude et al.}) = 0.07$ . For reaction (4) and (–4) the trend is different, in particular,  $k_4(\text{current study})/k_4(\text{Glaude et al.}) = 0.24$  and  $k_{-4}(\text{current study})/k_{-4}(\text{Glaude et al.}) = 0.45$ . Note that the species concentration is affected by both the forward and reverse reactions. The combination of all these new reaction rates gives more CO<sub>2</sub> under the experimental conditions. It should be clarified that our reaction rate calculations utilize updated thermodynamic data than used by Glaude et al.

Because of the large number of reaction pathways, a final recommendation for all the key individual reaction rates in the MB decomposition mechanism cannot yet be made, though direct measurements of certain reaction rates appear to be possible in the future and will definitely reduce some of the uncertainty in the mechanism development. The reason for the apparent failure of all models to capture the CO<sub>2</sub> yields at the very highest temperatures during MB pyrolysis is not yet known. However, it is clear that current model predictions based on the original Fisher et al. mechanism significantly underestimate the CO<sub>2</sub> yields during pyrolysis, while the improved MB model using the Huynh and Violi pyrolysis sub-model [5] with the new rates of the CH<sub>3</sub>OCO channels offers a significant improvement in the prediction of these same CO<sub>2</sub> yields.

#### 4. Conclusions

Measurements of CO<sub>2</sub> time-histories are carried out for methyl acetate, methyl propionate and methyl butanoate pyrolysis using diode laser absorption by CO<sub>2</sub> near 2.7 μm. High CO<sub>2</sub> yields during pyrolysis were found for all three methyl esters. The CO<sub>2</sub> yields were not strongly dependent on the alkyl chain length. Comparison of measured CO<sub>2</sub> concentration profiles and fractional yields from the MB experiments with three existing models of MB pyrolysis reveals that all models underestimate the CO<sub>2</sub> yield. A new MB model that combines the theoretical work of Huynh and Violi [5,14] and the Fisher et al. model [2] accurately recovers the experimentally observed CO<sub>2</sub> yields, except at the highest temperatures. The CO<sub>2</sub> time-history measurements provide new and stringent targets for the further development and validation of detailed mechanisms for methyl esters, and hopefully will lead to a better understanding of the effectiveness of methyl ester additives in reducing greenhouse gases and pollutant emissions.

The use of diode laser absorption near 2.7 μm provides improved sensitivity and accuracy for quantitative CO<sub>2</sub> time-history measurements, particularly in shock tubes, over the bands near 1.5 and 2.0 μm used previously to sense CO<sub>2</sub> in combustion gases. Using this new diagnostic method we plan to extend these measurements to the study of CO<sub>2</sub> yields in higher methyl esters and other oxygenated species. This diagnostic method complements the existing mid-IR fuel and UV-visible radical intermediate species time-history measurements in our fundamental shock tube kinetic database program [18], thereby contributing towards our goal of creating a complete description of the chemical history of critical combustion processes.

#### Acknowledgments

We gratefully acknowledge support from the Army Research Office (ARO) with Dr. Ralph Anthenien Jr. as technical monitor, the Air Force Office of Scientific Research (AFOSR) with Dr. Julian Tishkoff as technical monitor, and the Global

Climate and Energy Project at Stanford University. The research performed by Huynh and Violi is supported by the Air Force Office of Scientific Research (Grant No. FA9550-06-1-0376).

#### References

- [1] M.J. Hass, K.M. Scott, T.L. Alleman, R.L. McCormick, *Energy Fuels* 15 (2001) 1207–1212.
- [2] E.M. Fisher, W.J. Pitz, H.J. Curran, C.K. Westbrook, *Proc. Combust. Inst.* 28 (2000) 1579–1586.
- [3] W.K. Metcalfe, S. Dooley, H.J. Curran, J.M. Simmie, A. El-Nahas, M.V. Navarro, *J. Phys. Chem.* 111 (2007) 4001–4014.
- [4] S. Gail, M. Thomson, S.M. Sarathy, et al., *Proc. Combust. Inst.* 31 (2006) 3005–3011.
- [5] L.K. Huynh, A. Violi, *J. Org. Chem.* 73 (2008) 94–101.
- [6] O. Herbinet, W.J. Pitz, C.K. Westbrook, *Combust. Flame* 154 (2008) 507–528.
- [7] C.K. Westbrook, W.J. Pitz, H.J. Curran, *J. Phys. Chem.* 110 (2006) 6912–6922.
- [8] H.J. Curran, E.M. Fisher, P.-A. Glaude et al., *SAE paper* 2001-01-0653.
- [9] K.G.P. Sulzmann, D.E. Baxter, M. Khazra, T.S. Lund, *J. Phys. Chem.* 89 (1985) 3561–3566.
- [10] A. Farooq, H. Li, J.B. Jeffries, R.K. Hanson, *AIAA Joint Propulsion Conf.* 43 (2007), AIAA-2007-5015.
- [11] A. Farooq, J.B. Jeffries, R.K. Hanson, *Appl. Phys. B* 90 (2008) 619–628.
- [12] J.T. Herbon, R.K. Hanson, D.M. Golden, C.T. Bowman, *Proc. Combust. Inst.* 29 (2002) 1201–1208.
- [13] M.A. Oehlschlaeger, D.F. Davidson, R.K. Hanson, *J. Phys. Chem. A* 108 (2004) 4247–4253.
- [14] <<http://www.umich.edu/~avioli/mechs.html>>.
- [15] P.A. Glaude, W.J. Pitz, M.J. Thomson, *Proc. Combust. Inst.* 30 (2005) 1111–1118.
- [16] L.R. McCunn, K.C. Lau, M.J. Krisch, L.J. Butler, J.-W. Tsung, J.J. Lin, *J. Phys. Chem. A* 110 (2006) 1625–1634.
- [17] P.Y. Ayala, H.B. Schlegel, *J. Chem. Phys.* 108 (1998) 2314–2325.
- [18] Downloadable versions of the “Fundamental Kinetic Database Using Shock Tube Measurements” can be found at <<http://hanson.stanford.edu/news.htm>>.
- [19] P. Osswald, U. Struckmeier, T. Kasper, et al., *J. Phys. Chem. A* 111 (2007) 4093–4101.
- [20] W.R. Schwartz, C.S. McEnally, L.D. Pfefferle, *J. Phys. Chem. A* 110 (2006) 6643–6648.